Ann. Occup. Hyg., 2015, Vol. 59, No. 4, 514–524
doi:10.1093/annhyg/meu115
Advance Access publication 12 January 2015

BOHS
The Chartered Society for Worker Health Protection

Characterization of Size-Specific Particulate Matter Emission Rates for a Simulated Medical Laser Procedure—A Pilot Study

Ramon Lopez[1*], Steven E. Lacey[1], Julia F. Lippert[2], Li C. Liu[3], Nurtan A. Esmen[2] and Lorraine M. Conroy[2]

1. Department of Environmental Health Science, Richard M. Fairbanks School of Public Health, Indiana University, 714 N. Senate Ave., Indianapolis, IN 46202, USA
2. Division of Environmental and Occupational Health Sciences, School of Public Health, University of Illinois at Chicago, 2121 W. Taylor St., Chicago, IL 60612, USA
3. Division of Epidemiology and Biostatistics, School of Public Health, University of Illinois at Chicago, 1603 W. Taylor St., Chicago, IL 60612, USA
*Author to whom correspondence should be addressed. Tel: +1-317-278-0396; fax: +1-317-274-3443; e-mail: lopezram@iu.edu
Submitted 4 April 2014; revised 18 November 2014; revised version accepted 29 November 2014.

ABSTRACT

Prior investigation on medical laser interaction with tissue has suggested device operational parameter settings influence laser generated air contaminant emission, but this has not been systematically explored. A laboratory-based simulated medical laser procedure was designed and pilot tested to determine the effect of laser operational parameters on the size-specific mass emission rate of laser generated particulate matter. Porcine tissue was lased in an emission chamber using two medical laser systems (CO_2, $\lambda = 10\,600$ nm; Ho:YAG, $\lambda = 2100$ nm) in a fractional factorial study design by varying three operational parameters (beam diameter, pulse repetition frequency, and power) between two levels (high and low) and the resultant plume was measured using two real-time size-selective particle counters. Particle count concentrations were converted to mass emission rates before an analysis of variance was used to determine the influence of operational parameter settings on size-specific mass emission rate. Particle shape and diameter were described for a limited number of samples by collecting particles on polycarbonate filters, and photographed using a scanning electron microscope (SEM) to examine method of particle formation. An increase in power and decrease in beam diameter led to an increase in mass emission for the Ho:YAG laser at all size ranges. For the CO_2 laser, emission rates were dependent on particle size and were not statistically significant for particle ranges between 5 and 10 μm. When any parameter level was increased, emission rate of the smallest particle size range also increased. Beam diameter was the most influential variable for both lasers, and the operational parameters tested explained the most variability at the smallest particle size range. Particle shape was variable and some particles observed by SEM were likely created from mechanical methods. This study provides a foundation for future investigations to better estimate size-specific mass emission rates and particle characteristics for additional laser operational parameters in order to estimate occupational exposure, and to inform control strategies.

KEYWORDS: emission rate; laser generated particulate matter; medical laser; particulate matter; scanning electron microscopy; size-selective air sampling

INTRODUCTION

The US Occupational Safety and Health Administration (OSHA) estimated that over 500 000 health care professionals, including surgeons, nurses, anesthesiologists, and surgical technologists, were exposed to laser or electrosurgical smoke in 2008 (OSHA, 2008); with development of new medical laser applications increasing rapidly, the number of exposed health care professionals will only increase. Animal studies have suggested adverse health outcomes from the inhalation of laser generated air contaminants (LGAC), including pulmonary inflammatory response (Baggish and Elbakry, 1987; Freitag *et al.*, 1987; Baggish *et al.*, 1988) and pathological changes similar to interstitial pneumonia, bronchiolitis, and emphysema (Baggish and Elbakry, 1987; Wenig *et al.*, 1993). Cases have also been reported linking viral infection of health care professionals to inhalation of viable LGAC material (Hallmo and Naess, 1991; Calero and Brusis, 2003), and both OSHA and the National Institute for Occupation Safety and Health (NIOSH) have recognized the potential hazard that LGAC might pose to health care professionals and have recommended best practices during medical laser procedures (NIOSH, 1990; OSHA, 2008).

Little is known about the make-up and composition of laser surgical smoke, particularly regarding the concentration and size fraction of the particles (Council on Scientific Affairs, 1986; Kunachak and Sobhon, 1998). Particulate matter concentration in operating rooms during laser procedures have been estimated to be 3-fold higher than background and 100-fold higher than non-clinical office space (Tanpowpong and Koytong, 2002). Respirable

Table 1. Previous studies measuring particle size during tissue ablation

Laser type	Target material	Operational parameter settings	Reported particle statistics	Particle size range	Measurement technique	Reference
CO_2	Human laryngeal papillomas	P: 10 W[a], CW[b]	Mean: 0.80 μm	0.5–27μm	0.45 μm pore size filter attached to smoke evacuator	Kunachak and Sobhon (1998)
CO_2	Human Endometrial Tissue	P: 15–30 W[a], BD: 0.5 mm[c], PRF: 1.7 Hz[d]	Median: 0.31 μm	0.1–80 μm	Cascade impactor	Nezhat *et al.* (1987)
Nd-YAG	Sheep Bronchial Tissue	P:15–75 W[a]	Mean: 0.54 μm	Not specified	Cascade impactor	Freitag *et al.* (1987)
Excimer	Bovine Corneas	F: 100 mJ cm^{-2} [e]	Mean: 0.15 μm at 150 μm from target	Not specified	Raman spectra	Hahn *et al.* (1995)
Excimer	Human Eyes	BD:6.0 mm[c], PRF: 6 Hz[d], F: 160 mJ cm^{-2} [e]	Mean: 0.22 μm	0.13–0.42 μm	0.25 μm pore size methylcellulose filter attached to smoke evacuator	Taravella *et al.* (2001)

[a]P: power.
[b]CW mode: continuous wave mode laser.
[c]Beam diameter.
[d]PRF: pulse repetition frequency.
[e]F: fluence.

particulate matter concentration near the surgical site was measured between 30 and 1690 μg m^{-3}, and concentrations decreased rapidly with increased distance from the surgical site and with time after completion of lasing activity, dependent on the ventilation of the space (Tanpowpong and Koytong, 2002; Albrecht *et al.*, 1995). The average diameter of these medical laser generated particles has been reported between 0.1 and 0.8 μm (Table 1; Hahn *et al.*, 1995; Kunachak and Sobhon, 1998). Viewing LGAC with a scanning electron microscope (SEM), most particles fall within the fine and ultrafine particle size range (diameter < 0.1 μm) (Nezhat *et al.*, 1987; Hahn *et al.*, 1995; Taravella *et al.*, 2001). Ultrafine particles may be the most abundant in the laser plume, have little mass, and are difficult to count and measure leading to difficulty in particle size and concentration estimations (Nezhat *et al.*, 1987; Hahn *et al.*, 1995; Taravella *et al.*, 2001). Further, methods and materials used for collection and analysis of the medical laser generated plume differed between the studies, making comparison difficult. No studies have systematically examined the size-specific emission rate of medical laser generated particulate matter (LGPM) relative to laser operational parameters. Identifying the operational parameters that influence size-specific mass emission rates may help the clinical and occupational hygiene communities make informed decisions about risk and control strategies, and inform medical laser manufacturers in the design of systems that minimize or eliminate particle emissions. The objective of this pilot study was to determine size-specific mass emission rates of LGPM across a range of operational parameters and to photograph the generated particulate matter using an SEM.

METHODS

Emission chamber system design

An emission chamber was designed, built and evaluated for performance and capture of LGPM during a simulated medical laser procedure; a technical drawing of the chamber is provided in Fig. 1. A full description is reported elsewhere (Lippert *et al.*, 2014), but briefly, the chamber consisted of a square glass hood connected via a stainless steel transition section to an aluminum straight duct, and exhausted to a laboratory fume hood. Sampling probes for two real time particle counters were spaced 2.5 cm from each other and were located ~10 duct diameters (107 cm) downstream of the transition to allow the airstream to mix, stabilize, and reach laminar airflow. The AeroTrak® 8220 (TSI® Inc., Shorewood, MN, USA) measured particles larger than 0.3 μm in diameter at 6 size ranges (0.3–0.5, 0.5–1.0, 1.0–3.0, 3.0–5.0, 5.0–10, and >10 μm), and the P-Trak® 8525 (TSI® Inc.) ultrafine condensation particle counter measured particles between 0.02 and 1 μm. Isokinetic sampling, normally required when sampling particles in a gas, was not achieved due to the inability of the particle counter pumps to overcome the pressure difference necessary to match the airflow in the duct, so particle loss due to sampling in non-isokinetic conditions was calculated for each size fraction using a sampling error calculation for a properly aligned probe described by Hinds (1999). A ten percent loss was expected at the 10 μm size range, 4.4% at 5 μm and <2% for smaller particle size ranges. Results were adjusted to reflect the particle loss (Hinds, 1999). Size specific particle counts may also be affected by agglomeration and aging of particles during transport, but little is known about the behavior of LGPM after

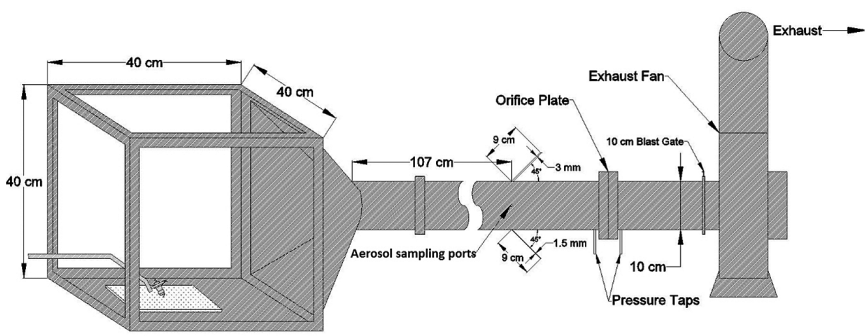

Figure 1 Emission chamber technical drawing.

generation, and we did not account for these behaviors in our study.

Two medical laser systems were used in the simulated medical laser procedure: the Ultra MD™ 40 Laser System (max power = 40 W, λ = 10 600 nm, pulsed; Laser Engineering Inc., Franklin, TN, USA) and the Medilas H 20-W Ho:YAG laser System (max power = 20 W, λ = 2100 nm, pulsed; Dornier Medtech, Germany). The Ho:YAG laser is commonly used in urological applications, while the CO_2 laser is used in almost all medical specialties (Pierce *et al.*, 2011).

We used porcine tissue in our laboratory simulation because of its similarity to human skin, its use in previous LGAC studies, (Stocker *et al.*, 1998; Plappert *et al.*, 1999) and its accessibility and low cost. Porcine tissue was purchased from a local butcher.

Experimental design

Three laser parameters were evaluated at settings that reflected the operational range for each device: power (W), beam diameter (mm), and pulse repetition frequency (PRF, in Hz; Table 2). To minimize the number of experiments for this pilot study, a 2^3 fractional factorial design was used, consisting of eight unique experiments (Table 3). Two replicate center-points were utilized to test the linearity of relationship (StatSoft, Inc., 2003; Kutner *et al.*, 2004). A test of curvature was conducted and the standard deviation of the center-points was used as the experimental error of the design. Matched background samples were taken prior to each experimental sample.

Experimental runs were replicated three times to characterize the variability within each operational parameter combination, and the order of each experimental run was randomized and performed over the course of 2 days. Three-factor ANOVA without interaction terms was used to test effects of the three operational parameters using SAS 9.2 (Cary, NC, USA) statistical software. Interaction terms were omitted from our analysis due to the small sample size. An *F*-test of significance was used to indicate if the mean emission rates for each operational parameter were statistically significantly different from each other.

Experimental procedure

The AeroTrak® and P-Trak® devices were zeroed each day before sampling using a HEPA Zero Filter. Background particle concentration in the laboratory was determined prior to each experimental run by sampling in the exhaust duct of the emission chamber with the Aerotrak® and P-Trak® devices for 10 min with the blower running but without lasing.

The Ho:YAG laser was prepared by attaching the laser fiber to a fiber tip holder to control the beam during lasing. The CO_2 laser was designed with a movable arm and did not require a fiber tip holder to control the beam. In both laser systems, the beam diameter was regulated using a metal prong attached to the laser arm or the fiber tip holder to control distance to the target tissue, and the lasing was performed at a rate of 2 mm s^{-1} (Lippert *et al.*, 2014).

Volumetric flow-rate in the straight duct was set to 3.3 m^3 min^{-1} to prevent saturation of the particle counters. Both particle counters began to log data 10 s after lasing had commenced and sampled for 10 min while lasing was ongoing, logging one measurement per second. The AeroTrak® particle counter recorded an average particle count per cubic meter of air sampled in each size range. The P-Trak® recorded a minimum, maximum, and average particle count per cubic centimeter of air sampled.

The generated particle emission rate was calculated by subtracting the background emission rate from the measured sample emission rate. Size-specific particle emission rates (particles min^{-1}) were calculated by

Table 2. Range of possible laser parameter settings, and parameter setting levels tested

	Variables	Power (W)	Beam diameter (mm)	Pulse repetition frequency (Hz)
CO_2 laser	Laser parameter range	1–40	0.5–2	1.2–5
	Parameter level (low; med; high)	(5; 8; 12)	(2; 1.25; 0.5)	(1.2; 3.2; 5)
Ho:YAG laser	Laser parameter range	1–20	0.5–5	1–20
	Parameter level (low; med; high)	(5; 8; 12)	(5; 3; 1)	(5; 8; 12)

Table 3. Operational parameter level settings for each experiment

	Operational parameter combinations	Power (W)	Beam diameter (mm)	Pulse repetition frequency (Hz)
	1	Low	High	Low
CO_2 laser	2	Low	Low	Low
	3	Low	High	High
	4	Low	Low	High
	5	High	High	Low
	6[a]	High	Low	Low
	7	High	High	High
	8[a]	High	Low	High
	Center-point	Med	Med	Med
Ho:YAG laser	1	Low	High	Low
	2	Low	Low	Low
	3	Low	high	High
	4	Low	Low	High
	5	High	High	Low
	6[a]	High	Low	Low
	7	High	High	High
	8[a]	High	Low	High
	Center-point	Med	Med	Med

[a]Filter sample for electron microscope characterization collected at selected combination.

multiplying the particle concentration by the volumetric flow-rate in the duct. Particle count emission rates were converted to mass emission rates for particles with diameters <10 μm. We assumed all particles measured were spheres and of unit density (1000 kg m^{-3}). For each particle size range, a representative particle diameter and corresponding mass was determined, then multiplied by the total number of particles in the size range, yielding the total mass of particles. The approach was to calculate the settling velocity for the largest and smallest particles in each size range, and determine the average value. The slip correction factor was applied to particles <1.0 μm in diameter. The particle mass associated with the mean settling velocity in each size range was then used as the representative particle mass. We chose the aerodynamic diameter for determining the size of the average particle and its representative mass because other methods, such as taking the mean diameter at each size range, greatly over-estimated the mass of the smallest size range (0.02–1 μm). For all other size-ranges, the mass emission rate calculate using the aerodynamic diameter was similar to the emission rate calculated using the median diameter. Particles >10 μm in diameter were not converted to mass emission rates and were not reported since the size range did not contain an upper bound.

Scanning electron microscopy

Medical laser generated particles from four parameter combinations that generated different size-specific

mass emission rates (Table 3) were collected on 37 mm SKC polycarbonate filters with a pore size of 0.8 μm in open-face cassettes. The sample air flow was 2.8 l min^{-1} and the sample duration was 20 s. The cassettes were held 2 cm from the surface of the porcine skin in a sampling methodology described by Taravella *et al.* (2001). Filters were desiccated for 24 h post-sampling prior to photographing high density areas using a Hitachi S3000-N SEM at a resolution of between 100× and 2000× in variable pressure mode (10 Pa) and at an acceleration voltage of 20 kV. Higher resolution was not used since the smallest particles were scattered and imaging any specific area would produce one or two particles at best, and only after searching the filter sample for a long period of time. Photographs were taken in filter areas of high particle density to examine particle shape and size, and to determine the mechanism of particle formation.

RESULTS

Background measurements

High variability was present at every size range, and at almost all of the size ranges the standard deviation was larger than the average. Graphical representations of the background variance by time of sample indicated higher variability for samples taken in the afternoon compared to the morning. However, when background emission rates were graphed by time and day of sample, most of the variability was between days rather than the time of day.

Emission rate results

In 43 of 377 (11%) samples, the adjusted emission rate was negative, indicating that the background emission rate was higher than the matched experimental sample and results were modified by replacing negative adjusted emission rates with an insignificantly small value of 100 particles per minute, converting the particle count concentration to a mass concentration and analyzing the data using the modified dataset (Table 4). Each particle size range followed a unique multimodal distribution, suggesting a mixture of influence from different mechanisms of particle formation, and simple transformations, including log and exponential transformations, did not improve the distributions of the data. The standard deviation between replicates of each parameter combination ranged between 0.5 and 125% of the mean for the Ho:YAG laser experiments, and from 0 and 200% for the CO_2 experiments.

The mean mass emission rate at each operational parameter level and the influence of each operational parameter on the emission of LGPM as described by percent variability (i.e. sum of squares of the operational parameter divided by sum of squares total) is presented in Table 5. For the Ho:YAG laser, an increase in power led to a significant increase in mass emission rates for all size ranges. A smaller beam diameter led to a significant increase in emission rate at every size range, and influence of the pulse repetition frequency was only statistically significant at the smallest particle size range. At all size ranges, beam diameter was the most influential parameter in the emission of LGPM, followed by power. Overall, the influence of the three operational parameters was highest in the emission of the smallest particles.

For the CO_2 laser, all three operational parameters were significantly influential in the mass emission of the smaller particle size ranges. Power was influential for particles <3.0 μm, beam diameter for particles <5.0 μm, and PRF was only influential at the smallest size range, 0.02–1 μm. Beam diameter was the most influential variable in the emission of LGPM at most particle size ranges, followed by power. Similar to the Ho:YAG laser, the influence of the three operational parameters on the emission of LGPM was highest for the smallest particles.

SEM results

We purposefully examined high particle density areas (Fig. 2) on each filter sample without determining actual concentration. The shape of particles changed as the diameter increased; particles <10 μm were generally spherical in shape, while larger particles were irregular. In filter samples from the Ho:YAG laser, small particles were observed more frequently (<1–10 μm) than in the CO_2 filter samples (<1 to >50 μm), but many particles observed in the Ho:YAG laser filter samples were fibers. The largest spherical particles appeared to be conglomerates or products of foam formation (Fig. 2B,D).

DISCUSSION

In the resultant emission rates using the Ho:YAG laser, an increase in power and a decrease in beam diameter led to statistically significant higher average mass

Table 4. Average size-specific mass emission rate (μg min^{-1}) for each operational parameter combination and corresponding standard deviation between replicate samples

Operational parameter combination		AeroTrak®					P-Trak®
		0.3–0.5 μm	0.5–1.0 μm	1.0–3.0 μm	3.0–5.0 μm	5.0–10.0 μm	0.02–1.0 μm
Ho:YAG laser	1	27 (11.7)	58 (32.0)	205 (108)	189 (115)	417 (263)	8.4×10^3 (60.4)
	2	0.9 (0.4)	1.4 (0.5)	4.6 (2.8)	3.0 (2.4)	4.9 (4.9)	5.6×10^2 (67.0)
	3	7.5 (2.9)	13 (5.3)	47 (16.7)	36 (13.3)	66 (29.1)	3.1×10^3 (45.5)
	4	0.4 (0.5)	0.3 (0.2)	1.3 (0.8)	1.1 (0.8)	1.9 (1.8)	4.9×10^2 (76.6)
	Center	27 (20.6)	25 (16.0)	74 (44.0)	58 (39.0)	120 (103)	6.0×10^3 (1.4×10^3)
	5	55 (27.1)	170 (128)	570 (400)	588 (479)	1212 (957)	1.5×10^4 (905)
	6	6.7 (4.8)	14 (8.0)	51 (30.7)	39 (23.2)	59 (35.2)	2.9×10^3 (922)
	7	111 (44.9)	177 (124)	532 (555)	550 (605)	1174 (1.1×10^3)	1.2×10^4 (1.8×10^3)
	8	12 (9.7)	11 (7.7)	25 (14.8)	19 (12.1)	30 (22.4)	3.2×10^3 (977)
CO_2 laser	1	0.1 (0.1)	0.1 (0.2)	0.2 (0.4)	0.0 (0.0)	0.0 (0.0)	1.8×10^1 (1.4)
	2	75 (63)	59 (51)	42 (1)	18 (16)	34 (32)	1.1×10^3 (968)
	3	0.2 (0.4)	0.1 (0.1)	0.3 (0.3)	0.2 (0.2)	0.3 (0.7)	1.9×10^2 (122)
	4	80 (89)	92 (140)	37 (45)	38 (54)	66 (104)	1.3×10^3 (1.8×10^3)
	Center	21 (20.8)	15 (19.3)	7.1 (5.5)	3.1 (2.7)	4.5 (4.5)	1.8×10^3 (2.9×10^3)
	5	1.9 (3.0)	1.0 (1.3)	1.9 (1.9)	0.9 (1.6)	1.0 (1.6)	2.5×10^2 (207)
	6	130 (87.7)	234 (201)	172 (138)	127 (103)	206 (177)	2.6×10^3 (1.8×10^3)
	7	80 (5.7)	53 (32.6)	23 (14.8)	10 (7.5)	14 (11.1)	3.7×10^3 (777)
	8	117 (30.5)	273 (178)	459 (323)	477 (498)	807 (931)	8.2×10^3 (5.3×10^3)

emission rates. With the CO_2 laser, power was statistically significant at size ranges <3.0 μm and beam diameter at size ranges <5.0 μm; PRF was only significant at the smallest size range (0.02–1 μm).

The percent variability each operational parameter explained suggests beam diameter was the most influential variable in the emission of LGPM and explained between 24.4 and 59.4% of the variability in the Ho:YAG laser and between 14.3 and 38.8% of the variability in the CO_2 laser. With both laser systems, the proportion of the variability explained by the parameters was greatest at the smallest particle size ranges, indicating the operational parameters influenced generation of the smallest particles the most.

Variability of the study design measured by the standard deviation of the center-points and of replicate samples was large. The results suggest future experimentation should involve additional replication, and improved control of the lasing experiments. Background samples in particular were highly variable when examined as a single data set. At most of the size ranges, the standard deviation was greater than the mean, indicating a deviation of at least 100%. Variability was mostly between days and not within day, indicating that the laboratory environment contributed significantly to the variation in background concentration. In future studies HEPA filtration of the incoming air would be helpful in decreasing background particle concentrations. The best solution would involve enclosing the chamber and supplying HEPA filtered air directly into the system, this would decrease the variability and concentration of particulate matter in the background airstream. Nevertheless, our pilot study was able to determine statistically

Table 5. Average background-corrected size-specific particle emission rate (μg min^{-1}) and percent variation explained by parameter setting

Operational parameter	Setting	AeroTrak®					P-Trak®
		0.3–0.5 μm	0.5–1.0 μm	1.0–3.0 μm	3.0–5.0 μm	5.0–10.0 μm	0.02–1.0 μm
Ho:YAG laser ($N = 29$)							
Power	12 W	46.1	93.8	294	299	619	8.3×10^3
	5 W	8.9	18	64.3	57	122	3.2×10^3
		$P < 0.002$	$P = 0.009$	$P = 0.028$	$P = 0.036$	$P = 0.033$	$P < 0.001$
% var. explained		20.7%	16.6%	13.0%	12.2%	12.2%	22.8%
Beam diameter	1 mm	50	104	338	340.8	717	9.9×10^3
	5 mm	5.0	7.0	20.5	15.6	23.9	1.8×10^3
		$P < 0.001$	$P = 0.001$	$P = 0.002$	$P = 0.005$	$P = 0.003$	$P < 0.001$
% var. explained		32.8%	31.1%	27.0%	24.2%	26.3%	59.4%
PRF	12 Hz	33	50.0	151.0	151.6	318.1	5.3×10^3
	5 Hz	22.3	60.7	207.5	204.8	423.3	6.3×10^3
		$P = 0.224$	$P = 0.896$	$P = 0.722$	$P = 0.787$	$P = 0.803$	$P = 0.037$
% var. explained		2.6%	0.0%	0.3%	0.2%	0.2%	3.5%
CO_2 laser ($N = 25$)							
Power	12 W	82.1	140.1	165.4	160.5	281.4	3.7×10^3
	5 W	35.7	34.6	18.3	13.4	25.3	7.0×10^2
		$P = 0.033$	$P = 0.025$	$P = 0.024$	$P = 0.076$	$P = 0.092$	$P = 0.002$
% var. explained		11.6%	14.4%	16.0%	11.3%	10.4%	29.4%
Beam diameter	0.5 mm	18.9	12.6	6.0	2.7	3.8	1.0×10^3
	2 mm	100.3	164.1	179.2	172.1	304.6	3.2×10^3
		$P = 0.004$	$P = 0.0018$	$P = 0.0085$	$P = 0.042$	$P = 0.049$	$P = 0.021$
% var. explained		38.8%	31.4%	22.7%	15.2%	14.6%	14.3%
PRF	5 Hz	64.0	96.3	120.8	126.6	224.2	3.0×10^3
	1.2 Hz	51.5	73.3	54.7	38.0	65.9	1.1×10^3
		$P = 0.383$	$P = 0.442$	$P = 0.197$	$P = 0.208$	$P = 0.221$	$P = 0.019$
% var. explained		1.8%	1.5%	4.8%	5.5%	5.3%	14.9%

significant changes in emission rates when varying the operational parameters.

Some additional factors that likely contributed to the variability in emission rates would also occur in the clinical setting and affect emission rates during procedures. Porcine tissue used varied in thickness, texture, and color, similar to findings in the literature (Yager and Scott, 1993; Avon and Wood, 2005), and similar to what occurs in clinical settings with patient variability.

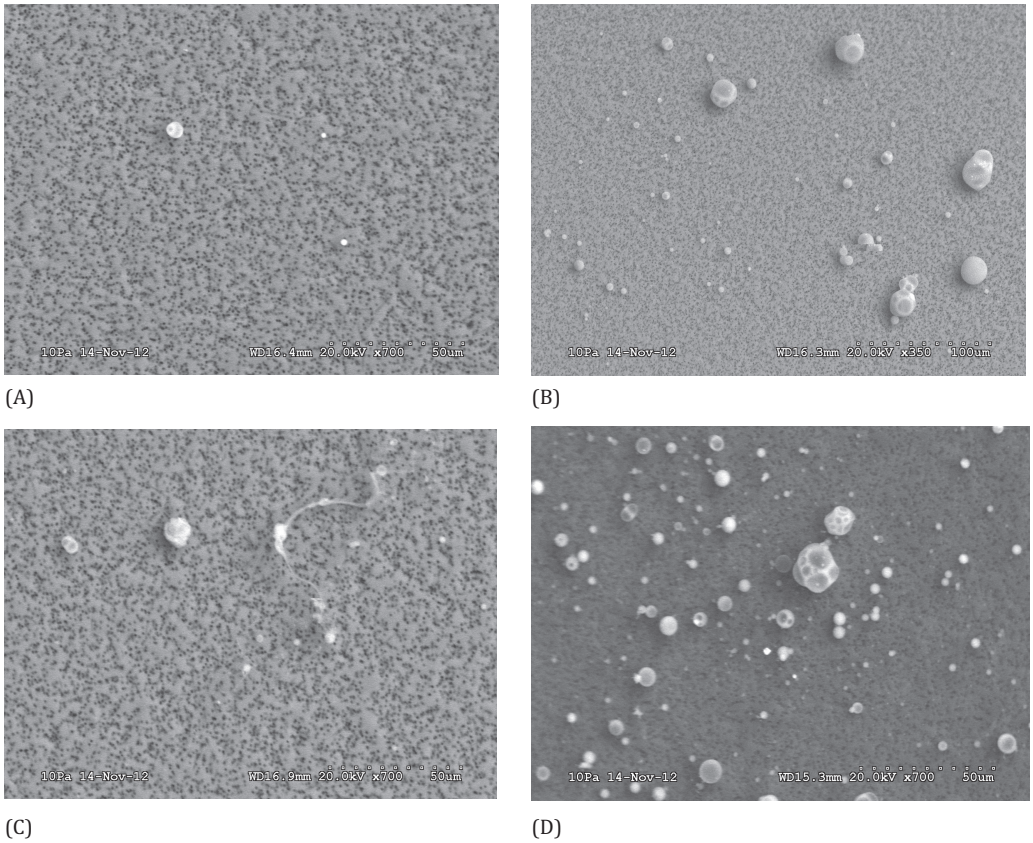

Figure 2 SEM photographs of high density areas from both laser devices and settings. (A) Filter from high PRF settings using the Ho:YAG laser. (B) Filter from high PRF settings using the CO_2 laser. (C) Filter from low PRF settings using the Ho:YAG laser. (D) Filter from low PRF setting using the CO_2 laser.

The operational parameter settings utilized in this pilot study were chosen to examine the influence of a range of settings on size-specific mass emission rates. Differences in delivery of the laser energy, maximum power, and PRF available for each laser did not allow for a direct comparison between laser systems. For example, pulse duration affects both power and pulse repetition frequency and may in turn affect the generation of LGPM. When power (W or J/s) is held constant, shorter pulse duration would increase the amount of energy (J) output by the laser. Higher energy per pulse is believed to increase a shockwave effect in tissue, increasing the amount of mechanically ejected material. In our study, the Ho:YAG laser did not allow for manipulation of the pulse duration, set by the manufacturer to 350 μs. The CO_2 laser did allow for limited manipulation, however, the shortest pulse duration available in the continuous setting was 0.1 s, over 280 times longer than for the Ho:YAG laser. This difference in pulse duration could have affected the size and amount of LGPM being generated by both laser devices. Regarding the laser systems used, the Ho:YAG laser delivered energy through a laser fiber that had to be periodically reshaped with use, which likely affected the power density on the tissue.

Imaging of particles using an SEM demonstrated a method to examine morphological differences in particles while varying laser operational parameter settings. Mechanism of formation may not definitely be determined by this study, but some particles could be generally categorized as products of mechanical ejection (i.e. physical tissue destruction) partially caused by a shockwave effect as opposed to combustion products, and are more likely to carry viable bacteria or viral particles. Many large particles in the CO_2 filter samples exhibited a uniform cratered surface that

was attributed to foam formation while larger particles from the Ho:YAG laser were irregularly shaped and included many fiber-like particles that may not be products of tissue-laser interaction, but hair from pig skin, particles from background air, or from contamination during filter preparation and transport. Direct comparison of filter samples to emission rate results was not possible, as areas of high concentrations were specifically chosen on each filter in order to maximize particle shapes and diameters for imaging. Many ultrafine or nano sized particles were noticed on filters, but the magnification we used was not sufficient to characterize these particles. Some studies have noted thermal damage to tissue can be mitigated with changes to wavelength, pulse duration, and irradiance. This may indicate that the mechanisms of formation and characteristics of LGPM will likely change with the manipulation of operational parameters (Walsh *et al.,* 1988; Ross *et al.,* 1996). Future research may involve collecting multiple filter samples at the same operational parameter combinations and randomly choosing areas on each filter to photograph and characterize. Since particle size varies considerably, and we noticed many particles in the nano size range on filters, photographs at higher magnifications should be taken. Similar images may be useful in determining the ability of particles to carry viable material and may be helpful in risk communication. Particles that are large in diameter and that are not from combustion products are more likely to carry viable cellular material and careful examination at high resolution may be able to distinguish bacteria, viruses, or complete cellular structures.

Expanding this study to include additional operational parameters such as pulse duration and energy per pulse may help to further explain particle generation, and ultimately identify operational parameters and settings that most influence the generation of particulate matter. Increasing the number of replicates will account for some of the experimental variability and allow testing of interaction terms, which may be influential contributors.

CONCLUSIONS

The goal of this pilot study was to establish a method of identifying laser operational parameters that influenced size-specific mass emission rates and to capture images of LGPM. Results indicate a need to further refine the collection methods by reducing the variability present in the study design and laboratory environment. We were able to demonstrate that all three factors were influential in the generation of particulate matter during the lasing procedure. An expansion and refinement of these methods would be helpful in determining clinical procedures and laser device settings that produce the greatest exposure risks, and communicating the risk to the clinical and occupational hygiene community will increase awareness and ultimately lead to improved control strategies and laser device design that minimize or eliminate LGPM exposures.

FUNDING

National Institute of Occupational Safety and Health pilot projects training grant program (T42/OH008672).

DISCLAIMER

Its contents, including any opinions and/or conclusions expressed, are those of the authors.
The authors declare no conflict of interest.

ACKNOWLEDGMENTS

The authors would like to thank Mr. Sal Cali and Dr. Anders Abelmann for their review of earlier versions of this manuscript, and Drs. John Breskey, Chiping Nieh and Rachael Jones for their advice during preparation of this manuscript.

REFERENCES

Albrecht H, Washce W, Muller GJ. (1995) Assessment of the risk potential of pyrolysis products in plume produced during laser treatment under OR conditions. Proceedings of SPIE. *Int Soc Optics Photonics*; 455–63.

Avon SL, Wood RE. (2005) Porcine skin as an in-vivo model for ageing of human bite marks. *J Forensic Odontostomatol*; 23: 30–39.

Baggish MS, Baltoyannis P, Sze E. (1988) Protection of the rat lung from the harmful effects of laser smoke. *Lasers Surg Med*; 8: 248–53.

Baggish MS, Elbakry M. (1987) The effects of laser smoke on the lungs of rats. *Am J Obstet Gynecol*; 156: 1260–65.

Calero L, Brusis T. (2003) Laryngeal papillomatosis—first recognition in Germany as an occupational disease in an operating room nurse. *Laryngorhinootologie*; 82: 790–3.

Council on Scientific Affairs. (1986) Lasers in medicine and surgery. *JAMA: the journal of the American Medical Association*; 256 900–07.

Freitag L, Chapman GA, Sielczak M *et al.* (1987) Laser smoke effect on the bronchial system. *Lasers Surg Med*; 7: 283–88.

Hahn DW, Ediger MN, Pettit GH. (1995) Dynamics of ablation plume particles generated during excimer laser corneal ablation. *Lasers Surg Med*; 16: 384–9.

Hallmo P, Naess O. (1991) Laryngeal papillomatosis with human papillomavirus DNA contracted by a laser surgeon. *Eur Arch Otorhinolaryngol*; 248: 425–27.

Hinds WC. (1999) *Aerosol technology*. New York: John Wiley & sons, Inc.

Kunachak S, Sobhon P. (1998) The potential alveolar hazard of carbon dioxide laser-induced smoke. *J Med Assoc Thai*; 81: 278–82.

Kutner MH, Nachtshein CJ, Neter J, Li W. (2004) *Applied linear statistical models*. New York: Mcgraw-Hill Irwin.

Lippert JF, Lacey SE, Lopez R *et al.* (2014) A pilot study to determine medical laser generated air contaminant emission rates for a simulated surgical procedure. *J Occup Environ Hyg*; 11: D69–D76.

Nezhat C, Winer WK, Nezhat F *et al.* (1987) Smoke from laser surgery: is there a health hazard? *Lasers Surg Med*; 7: 376–82.

NIOSH. (1990) NIOSH health hazard evaluation and technical assistance report. Cincinnati, OH: US Department of Health and Human Services; Report No.: HETA-88-101-2008.

OSHA. (2008) Safety and health topics: laser/electrosurgery plume. Available at: https://www.osha.gov/SLTC/laserelectrosurgeryplume. Accessed 30 July 2013.

Pierce JS, Lacey SE, Lippert JF *et al.* (2011) An assessment of the occupational hazards related to medical lasers. *J Occup Environ Med*; 53: 1302–9.

Plappert UG, Stocker B, Helbig R *et al.* (1999) Laser pyrolysis products-genotoxic, clastogenic and mutagenic effects of the particulate aerosol fractions. *Mutat Res*; 441: 29–41.

Ross EV, Domankevitz Y, Skrobal M *et al.* (1996) Effects of CO_2 laser pulse duration in ablation and residual thermal damage: implications for skin resurfacing. *Lasers Surg Med*; 19: 123–9.

StatSoft, Inc. (2003). *Electronic Statistics Textbook. Design of experiments: Science, Industrial DOE*. Tulsa, OK: StatSoft. Available at: http://www.Statsoft.com/textbook.

Stocker B, Meier T, Fliedner TM *et al.* (1998) Laser pyrolysis products: sampling procedures, cytotoxic and genotoxic effects. *Mutat Res*; 412: 145–54.

Tanpowpong K, Koytong W. (2002) Suspended particulate matter in an office and laser smoke particles in an operating room. *J Med Assoc Thai*; 85: 53–7.

Taravella MJ, Viega J, Luiszer F *et al.* (2001) Respirable particles in the excimer laser plume. *J Cataract Refract Surg*; 27: 604–7.

Walsh JT Jr, Flotte TJ, Anderson RR *et al.* (1988) Pulsed CO_2 laser tissue ablation: effect of tissue type and pulse duration on thermal damage. *Lasers Surg Med*; 8: 108–18.

Wenig BL, Stenson KM, Wenig BM *et al.* (1993) Effects of plume produced by the Nd:YAG laser and electrocautery on the respiratory system. *Lasers Surg Med*; 13: 242–45.

Yager JA, Scott D. (1993) The skin and appendages. In : Jubb, K, Kennedy, P, Palmer, editors. *Pathology of domestic animals*. San Diego: Academic Press, p. 220.